

# ERK5 MAPK Regulates Embryonic Angiogenesis and Acts as a Hypoxia-sensitive Repressor of Vascular Endothelial Growth Factor Expression\*

Received for publication, July 26, 2002, and in revised form, September 5, 2002  
Published, JBC Papers in Press, September 6, 2002, DOI 10.1074/jbc.M207573200

Sue J. Sohn, Brieana K. Sarvis, Dragana Cado, and Astar Winoto‡

From the Department of Molecular and Cell Biology, Division of Immunology and Cancer Research Laboratory, University of California, Berkeley, California 94720-3200

**During angiogenesis, endothelial cells undergo proliferation, reorganization, and stabilization to establish a mature vascular network. This process is critical for establishing a functional circulatory system during development and contributes to the pathological process of tumor growth. Here we report that embryos deficient for the ERK5 MAPK die between embryonic days 10.5 and 11.5 with angiogenic failure and cardiovascular defects. We show that ERK5 deficiency leads to an increased expression of the vascular endothelial growth factor (VEGF), dysregulation of which has been shown to impede angiogenic remodeling and vascular stabilization. Our data also reveal that ERK5 negatively regulates transcription from the *veg*f locus during hypoxic responses. Importantly, ERK5 is required at an earlier developmental stage than p38 $\alpha$ , and p38 $\alpha$  does not compensate for ERK5 deficiency. These results demonstrate that ERK5 plays a specific role in the regulation of early angiogenesis.**

Vasculogenesis and angiogenesis are two critical processes of establishing the cardiovascular system in vertebrate embryos. Vasculogenesis involves generation of the primitive vascular plexus from angioblasts that have recently differentiated from mesodermal tissues. This process leads to the formation of the early heart tube and major blood vessels such as the dorsal aorta (reviewed in Refs. 1–3). Subsequently, the process of angiogenesis drives maturation and elaboration of the primary vascular network via proliferation and migration of endothelial cells (2–5). Angiogenic remodeling involves sprouting and invasion of vessels into avascular sites as well as pruning and fusion of existing vessels. Unlike vasculogenesis, which is thought to occur only during early embryogenesis, angiogenesis occurs throughout development as well as in adult animals and is essential for wound healing and tumor growth (2–5).

*In vivo*, vasculogenic and angiogenic signals are controlled by tightly regulated interactions that occur between soluble factors and their receptors. The indispensable role of vascular endothelial growth factor (VEGF)<sup>1</sup> in early vasculogenesis has

been demonstrated in mice bearing a targeted mutation at the *veg*f locus (6, 7). Importantly, mutation of one allele is sufficient to disrupt normal vasculogenesis and cause lethality. It has also been shown that a mutation that results in a 2–3-fold increase in the level of VEGF causes embryonic lethality at midgestation due to cardiovascular failure (8). These results indicate that mouse embryos exhibit exquisite sensitivity to changes in the level of VEGF. VEGF also acts as an endothelial cell survival factor and a vascular permeability factor (9), and it has been postulated to regulate angiogenesis when acting in combination with other factors such as angiopoietin (Ang)-1 and -2 (reviewed in Ref. 10). Additional factors including tissue factor (11), platelet-derived growth factor (12), and transforming growth factor- $\beta$  (1) are also required for establishing a functional circulatory system in developing embryos.

In both developing embryos and tumor models, oxygen homeostasis plays an important role in regulating angiogenesis. For example, during retinal development in postnatal rodents, artificial perturbation of oxygen levels results in abnormal vascularization associated with dysregulation of VEGF (13–15). Increased VEGF expression in a hypoxic environment promotes vessel growth, but these vessels tend to be leaky and hemorrhagic, and they grow in disorganized patterns. These data further support the idea that VEGF must work in concert with other angiogenic factors to establish stable and organized vasculature. Similarly, localized hypoxic responses drive increased VEGF expression and angiogenesis in tumors (16).

It has been well documented that members of the mitogen-activated protein kinases (MAPKs) regulate diverse cellular functions (reviewed in Ref. 17). They have been shown to mediate proliferation, apoptosis, and differentiation depending on the stimuli and the cellular context. Activation of the MAPKs requires dual phosphorylation of a threonine and a tyrosine in their consensus TXY motif by MEKs (MAPK kinases), which in turn are phosphorylated and activated by their upstream MEKKs (MKKKs or MAPK kinase kinases). Multiple classes of MAPKs have thus been identified: ERK1/2, JNKs (also known as stress-activated protein kinases; JNK1, -2, and -3), p38 MAPKs ( $\alpha$ ,  $\beta$ ,  $\gamma$ , and  $\delta$ ), ERK3, ERK4, ERK5, ERK7, and p57 MAPKs (17). Most of these proteins are expressed widely, and many can perform overlapping functions in cells in *in vitro* systems. However, studies of several of these genes in knockout mouse models have pointed to a surprising degree of functional specificity among the MAPKs. For example, mice lacking ERK1

\* This work was supported by National Institutes of Health Grant CA66236 (to A. W.). The costs of publication of this article were defrayed in part by the payment of page charges. This article must therefore be hereby marked "advertisement" in accordance with 18 U.S.C. Section 1734 solely to indicate this fact.

‡ To whom correspondence should be addressed: Dept. of Molecular and Cell Biology, Division of Immunology and Cancer Research Laboratory, 465 Life Science Addition, University of California, Berkeley, California 94720-3200. Tel.: 510-643-3245; Fax: 510-642-0468; E-mail: winoto@uclink4.berkeley.edu.

<sup>1</sup> The abbreviations used are: VEGF, vascular endothelial growth factor; Ang, angiopoietin; MAPK, mitogen-activated protein kinase;

MEF2, myocyte enhancer factor-2; ES, embryonic stem; HIF-1, hypoxia-inducible factor 1; MEF, mouse embryonic fibroblast; ARNT, aryl hydrocarbon receptor nuclear translocator; MEK, mitogen-activated protein kinase/extracellular signal-regulated kinase kinase; MEKK, MEK kinase; ERK, extracellular signal-regulated protein; JNK, c-Jun N-terminal kinase; *En*, embryonic day *n*.

exhibit defects in thymocyte maturation without overt defects during embryonic development (18). Mice lacking JNK1 (19) or JNK2 (20) singly also exhibit specific defects in T-cell maturation and function, whereas mice doubly deficient for JNK1 and JNK2 die *in utero* (21). More recently, deficiency of p38 $\alpha$  was shown to result in embryonic lethality starting at E10.5, with vascular remodeling defects (22, 23), as well as defects in erythroid cell differentiation (24).

We and other investigators previously identified and characterized ERK5 (BMK1), a novel MAPK protein that contains a catalytic domain homologous to ERK1/2 and a unique carboxyl-terminal domain. ERK5 has been shown to be activated in response to serum (25), growth factors (26), neurotrophins (27, 28), and neuregulins (29), indicating that ERK5 regulates multiple cellular functions. ERK5 has been shown to activate myocyte enhancer factor-2 (MEF2) family transcription factors (specifically MEF2A, -C, and -D) in response to epithelial growth factor (30) and a combination of phorbol 12-myristate 13-acetate and ionomycin in T-cell lines (31). The MEF2 proteins interact with ERK5 (31, 32), and phosphorylation by ERK5 probably increases their transcriptional activity (30). Furthermore, we previously showed that ERK5 interacts with MEF2 proteins via its C-terminal domain, which also acts as a transactivator for MEF2-dependent transcription (31). Thus, ERK5 constitutes a unique class of MAPKs that can modify the activity of targets not only through phosphorylation but also through physical interactions, thereby invoking conformational changes in the target proteins and/or providing docking sites for additional components of transcriptional machinery.

To elucidate specific requirements for ERK5 *in vivo*, we generated mice lacking ERK5 by targeted gene disruption. We show that ERK5 plays indispensable, multifaceted roles in embryonic angiogenesis. ERK5 deficiency leads to phenotypes consistent with its purported role as an activator of MEF2 transcription factors. Moreover, we present data suggesting a role of ERK5 as a negative regulator of VEGF expression and as a sensor of oxygen homeostasis. Thus, ERK5 plays both positive and negative regulatory roles in controlling angiogenic signals.

#### EXPERIMENTAL PROCEDURES

**Generation and Analyses of *erk5*<sup>-/-</sup> Mice**—The *erk5* locus was disrupted in embryonic stem (ES) cells as described under "Results." Chimeric mice and ERK5<sup>+/-</sup> heterozygous mice were maintained in a specific pathogen-free facility. Most of the data presented in this study were obtained from mice retaining the *neo* cassette. However, identical results have been obtained using animals in which the *neo* cassette was eliminated (by crossing ERK5<sup>+/-</sup> mice with *cmv-Cre* transgenic mice).

**Southern Blot Analyses**—Genomic DNA from ES cells was prepared using standard protocols (33). To detect targeted mutation at the *erk5* locus, we resolved genomic DNA digested with *EcoRV* in agarose gels, blotted it onto nylon membranes, and hybridized with a radiolabeled 200-bp *HpaI/EcoRV* genomic fragment 5' of the targeting sequences. The presence of an *EcoRV* site within the Neo cassette of the mutant *erk5* allele results in a smaller, 3.5-kb *EcoRV* fragment detectable by the 5' probe. The wild-type endogenous *EcoRV* fragment is 5.5 kb.

**Anti-ERK5 Immunoblot Analyses**—Individual embryos at E9 were harvested and washed in cold phosphate saline buffer and lysed in ice-cold lysis buffer containing 1% Triton X-100 (50 mM Tris-HCl, pH 7.5, 150 mM NaCl, 1 mM phenylmethylsulfonyl fluoride, 1 mM Na<sub>3</sub>VO<sub>4</sub>, 1  $\mu$ g/ml aprotinin, 1  $\mu$ g/ml leupeptin). After the lysates were cleared by centrifugation at 4 °C, they were boiled in sample buffer (0.062 M Tris-HCl, pH 6.8, 2% SDS, 210% glycerol, 5%  $\beta$ -mercaptoethanol, 0.5 mg of bromophenol blue) for 10 min, placed on ice, and resolved by SDS-PAGE. The proteins were transferred onto nitrocellulose, blotted with affinity-purified anti-ERK5 rabbit polyclonal antibodies (31), incubated with horseradish peroxidase-conjugated anti-rabbit Ig (Amersham Pharmacia Biotech), and visualized by chemiluminescence using the Western Lightning kit (PerkinElmer Life Sciences).

**Genotype Determination of Embryos**—Genomic DNA was isolated from the yolk sacs that were dissected away from the decidual and

placental tissues, washed in phosphate saline buffer and lysis solution (10 mM Tris-HCl, pH 8.5, 1.5 mM MgCl<sub>2</sub>, 0.45% Nonidet P-40, 0.45% Tween 20), and digested in proteinase K (100  $\mu$ g/ml). Genotype was determined by setting up two separate PCRs. The wild-type allele was amplified with a forward primer (5'-GAA CAC TCA TCA CTG GGT TGG CAA-3') and a reverse primer (5'-GGT CTC GAT GAT CTC GTA CTC GTC-3'); the mutant allele was amplified with a neomycin-specific primer set (forward primer, 5'-TTC GGC TAT GAC TGG GCA CAA CAG-3'; reverse primer, 5'-TAC TTT CTC GGC AGG AGC AAG GTG-3').

**Whole Mount *In Situ* Hybridization**—Embryos were harvested at the indicated times and fixed in 4% paraformaldehyde overnight. *In situ* hybridization was performed using a standard protocol (34) with modifications. Briefly, fixed embryos were rehydrated through a series of ethanol exchanges, permeabilized in Proteinase K (10  $\mu$ g/ml in phosphate saline buffer), and refixed in 4% paraformaldehyde, 0.1% glutaraldehyde. Embryos were then hybridized with digoxigenin-labeled RNA probes that were transcribed with T7 RNA polymerase. The ERK5 antisense or sense probe was generated from a pBluescript (Stratagene, La Jolla, CA) plasmid containing a 1.9-kb *EcoRI* ERK5 cDNA insert. The dHAND and eHAND antisense probes were from Dr. E. Olson (35) via Dr. W. Skarnes. After hybridization, embryos were incubated in alkaline phosphatase-conjugated anti-digoxigenin Fab fragments (Roche Diagnostics), washed in maleic acid buffer (100 mM maleic acid, 150 mM NaCl, pH 7.5, 0.5% Tween 20), and developed by reaction with BM-Purple substrates (Roche Diagnostics). The photographs were taken with a Nikon N6006 camera attached to a Zeiss microscope, with equivalent exposure among different samples.

**Histology and Immunohistochemical Analyses**—Embryos were harvested and fixed in 4% paraformaldehyde or Bouin's solution (Sigma) overnight, embedded in paraffin using standard protocols, sectioned at 8- $\mu$ m thickness, and fixed onto Superfrost Plus microscope slides (Fisher). For the heart and placental sections, the slides were stained with hematoxylin and eosin. Whole mount immunohistochemical analysis of PECAM (CD31) expression was performed according to a standard protocol (34). Briefly, the embryos were fixed in Me<sub>2</sub>SO/methanol, bleached in hydrogen peroxide/Me<sub>2</sub>SO/methanol, and stained with purified anti-PECAM 1 antibody (MEC 13.3; BD Pharmingen, San Diego, CA) and were developed with the DAB peroxidase substrate kit (Vector Science, Burlingame, CA).

**RNA Purification and Semiquantitative RT-PCR**—Total RNA was isolated from individual embryos or pools of embryos combined by genotype following a standard LiCl precipitation protocol (34). 1  $\mu$ g of total RNA was reverse transcribed with oligo(dT)<sub>15</sub> primers (Promega, Madison, WI) and RT SuperScript (Invitrogen, Carlsbad, CA) to generate single-stranded cDNA templates. Semiquantitative RT-PCR for VEGF, angiopoietin (Ang)-1, Ang-2, Flt-1, Tie-1, Tie-2, and  $\gamma$ -actin was performed using the SYBR<sup>®</sup> Green system (PerkinElmer Life Sciences) and a GeneAmp<sup>®</sup> 5700 Sequence Detector (PerkinElmer Life Sciences). Standard curves were generated for each primer set with cDNA templates from ERK5<sup>+/+</sup> or ERK5<sup>+/-</sup> controls. The relative abundance of transcripts in unknown samples was determined by regression analyses based on these standard curves and was normalized against  $\gamma$ -actin. The sequences of primers used for RT-PCR are as follows: VEGF 302F, 5'-CAA GCC GTC CTG TGT GCC-3'; VEGF 352R, 5'-TCA TCG TTA CAG CAG CCT GC-3'; Ang-1 587F, 5'-CTC AGT GGC TGC AAA AAC TTG A-3'; Ang-1 637R, 5'-CCG ACT TCA TAT TTT CCA CAA TGT AAT-3'; Ang-2 1697F, 5'-TCT AAA TGC CTG CCT ACA CTA CCA G-3'; Ang-2 1747R, 5'-TTA ATC TTT GGA TGC CTA CAC TAC CAG-3'; Flt1 2483F, 5'-AGC CTA CCT CAC CGT GCA AG-3'; Flt1 2538R, 5'-GCG TGA TCA GCT CCA GGT TT-3'; Tie1 1527F, 5'-GCA CCA TGC TTT TGT CTA CCA A-3'; Tie1 1577R, 5'-CTG TGG TCC TGT CTG GCT CC-3'; Tie2 644F, 5'-GTG CTT ATT TCT GTG AAG GTC GAG T-3'; Tie2 694R, 5'-TCC GTA TCC TTA TAG CCT GTC CTC-3';  $\gamma$ -Actin5, 5'-GCA CCT AGC ACG ATG AAG ATT AAG-3';  $\gamma$ -Actin3, 5'-GCC ACC GAT CCA GAC TGA GT-3'.

**Culture of Dissociated Embryo Cells and VEGF ELISA**—Individual E9.5 embryos were harvested using sterile techniques, washed with sterile phosphate saline buffer, and dissociated by trypsinization and mechanical shearing. The cells were counted, and 2  $\times$  10<sup>5</sup> cells from each embryo were cultured in Dulbecco's modified Eagle's medium containing 15% fetal calf serum and supplemented with penicillin/streptomycin, L-glutamine, sodium pyruvate, nonessential amino acids, and  $\beta$ -mercaptoethanol and buffered with HEPES. On day 2 of culture, the cells were split into duplicate samples, and the following day one set was placed in a modular incubator chamber that had been flushed with a hypoxic gas mixture containing 94% N<sub>2</sub>, 5% CO<sub>2</sub>, 1% O<sub>2</sub> and further cultured at 37 °C for 24 h. The culture supernatants were collected, and

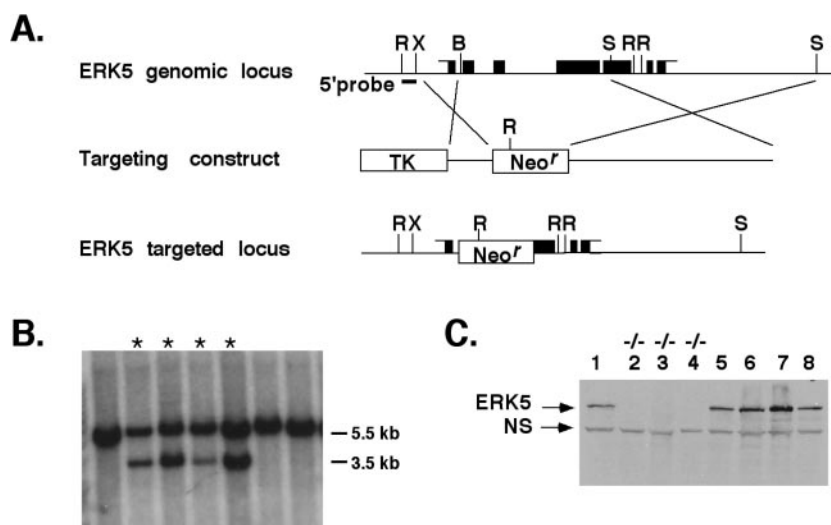


**FIG. 1. Targeted disruption of the *erk5* gene.** *A*, the *erk5* genomic locus is shown with select restriction sites and the exon-intron boundaries. The targeting vector contains a thymidine kinase gene (*TK*) and the *XhoI/BamHI* and the *SpeI* fragments flanking the neomycin resistance cassette (*Neo<sup>r</sup>*). Integration of this construct by homologous recombination at the *erk5* locus eliminates exons 2–4 and part of exon 5. *R*, *EcoRV*; *X*, *XhoI*; *B*, *BamHI*; *S*, *SpeI*. *B*, Southern blot analyses of the ES clones. Genomic DNA from multiple ES clones was digested with *EcoRV* and probed with the 5' probe, corresponding to a 200-bp *RX* genomic fragment (shown in *A*). The 3.5-kb fragment corresponds to the targeted allele, and the 5.5-kb fragment corresponds to the wild-type allele. \*, clones possessing the mutation. These clones were confirmed by digestion with *XhoI* and hybridization with a 3' probe (data not shown). *C*, anti-ERK5 immunoblot analysis of total lysates from E9.0 embryos indicates that the homozygous-null mutants lack ERK5 proteins (lanes 2–4). NS, a nonspecific signal.

the VEGF concentrations were determined by ELISA using a kit (Quantikine™ M, mouse VEGF immunoassay; R&D Systems), according to the manufacturer's instructions.

**Generation of Mouse Embryonic Fibroblast (MEF) Lines, Transfection, and VEGF Luciferase Assay**—Embryos were harvested on E9.5, dissociated as described above, and cultured in complete Dulbecco's modified Eagle's medium containing 15% fetal calf serum. The cells were passed at confluence until they went through crisis. To monitor the VEGF promoter (pVEGF) activities, 1–2  $\mu$ g of pVEGF-Luc (gift from Dr. B. Z. Levi, Weizmann Institute of Science, Israel), together with increasing amounts (0, 2, or 4  $\mu$ g) of ERK5 cDNA plasmid (pCI ERK5) (31), was transiently transfected into MEFs using FuGene6 reagent (Roche Diagnostics), following the manufacturer's recommended protocol. Where indicated, 1  $\mu$ g each of pCEP4 HIF-1 $\alpha$  (gift from Dr. G. Semenza, Johns Hopkins University) and pcDNA3-ARNT (HIF-1 $\beta$ , gift from Dr. E. Huang via Dr. M. Rubinstein, Weizmann Institute of Science, Israel) was co-transfected. A *Renilla* luciferase plasmid (pEFRL) was co-transfected as a normalizing control. Transfections were performed in duplicate, and one set was placed in a hypoxic chamber (as described above) 24 h after transfection and was cultured under hypoxia for additional 24 h. Luciferase activities were measured using the Dual-Luciferase Assay System (Promega, Madison, WI) and read by a Monolight 2010 Luminometer (Analytical Luminescence Laboratory, Ann Arbor, MI).

## RESULTS

**Generation of ERK5-deficient Mice**—We isolated and characterized several overlapping clones containing the ERK5 gene from a 129sv mouse genomic library. Restriction digest and DNA sequencing analyses revealed that the ERK5 gene is encoded by seven exons and six introns spanning ~5.5 kb. The targeting construct was generated by replacing the 3.7-kb *BamHI-SpeI* genomic fragment with a neomycin resistance cassette (Fig. 1*A*), eliminating a region that corresponds to 1.8 kb of coding sequence and includes the translation initiation and the kinase domain. The linearized construct was electroporated into ES cells, and colonies that survived the standard G418/gancyclovir double selection were analyzed for homologous recombination by Southern blotting. We generated chimeric mice from three independent ES clones possessing the targeted allele (Fig. 1*B*). These mice were subsequently bred onto the C57BL/6 background to generate ERK5<sup>+/-</sup> heterozygotes.

**ERK5<sup>-/-</sup> Embryos Die in Utero**—Genotype analyses of mul-

iple litters of ERK5<sup>+/-</sup> intercrosses indicated that no ERK5<sup>-/-</sup> mice were born. Timed mating analyses clearly demonstrated that ERK5<sup>+/+</sup>, ERK5<sup>+/-</sup>, and ERK5<sup>-/-</sup> embryos are present at the expected Mendelian ratios up to E10.5 during embryonic development (Table I). However, the viability of ERK5<sup>-/-</sup> embryos starts to decline around E10, and they do not survive beyond E11. Thus, embryonic lethality of ERK5 deficiency is 100% penetrant by E11.5. As shown in Fig. 1*C*, an anti-ERK5 immunoblotting analysis demonstrates the absence of ERK5 proteins in homozygous embryos (lanes 2–4), confirming functional disruption of the *erk5* gene. During these analyses, we observed that ERK5<sup>-/-</sup> embryos were indistinguishable from their littermate controls up to E9 (Fig. 2*A*, top panels). Beginning at E9.5, some of the ERK5<sup>-/-</sup> embryos appear paler and smaller than the ERK5<sup>+/+</sup> or ERK5<sup>+/-</sup> controls (Fig. 2*A*, middle panels). At E10 and after, all ERK5<sup>-/-</sup> embryos exhibit stunted growth, especially in the head and the lower trunk regions, and many also exhibit dilated pericardial sacs (Fig. 2*A*, bottom panels) that occasionally show signs of hemorrhage. The yolk sacs of ERK5<sup>-/-</sup> embryos also appear pale or contain interconnected vasculature at E9.5 (Fig. 2*B*, upper panels). Red blood cells are generated and found in both yolk sacs and in the embryo proper, indicating that amalgamation of extraembryonic and embryonic circulation occurs successfully. By E10, the blood vessels found in the control yolk sacs undergo extensive remodeling and arborization to form distinct large and branching vessels (Fig. 2*B*, lower left panel). In contrast, the surfaces of the ERK5<sup>-/-</sup> yolk sacs become pale and smooth except for intermittent, diffuse patches of red blood cells, and the primitive vessels that form around E9–E9.5 dissipate (Fig. 2*B*, lower right panel).

**ERK5<sup>-/-</sup> Embryos Exhibit Vascular/Angiogenic Defects**—To further evaluate the impact of ERK5 deficiency on vascular development, we performed whole-mount immunohistochemical analyses for the endothelial cell marker CD31 (PECAM) at E9, E9.5, and E10. As shown in Fig. 3*A*, the organization of the CD31-expressing endothelial cells appears normal in the heart (in the endocardium) and in dorsal aorta at E9 (panels *a* and *b*), suggesting that the formation of primary vasculature is unaffected. Initial vascularization also takes place in the yolk sacs,

TABLE I  
Summary of timed pregnancy analyses of the  $ERK5^{+/-} \times ERK5^{+/-}$  intercrosses

The percentage of each genotype is indicated in parentheses. Viability was assessed by the presence of the heartbeat. At E11.5, the genotypes of resorbing embryos (\*) were determined from the yolk sac genomic DNA. No viable embryos were recovered at E11.5 and beyond. At E12.0, only remnants of resorbing bodies were present, and the genotypes of these embryos could not be determined.

Embryonic day	Genotype			Total embryos	Viability of -/- embryos
	+/+	+/-	-/-		
E8.5	18 (23%)	47 (59%)	15 (19%)	80	% 100
E9.0	38 (26%)	75 (52%)	31 (22%)	144	100
E9.5	35 (32%)	54 (49%)	22 (20%)	111	100
E10.0	7 (16%)	23 (52%)	14 (32%)	44	97
E10.5	7 (24%)	13 (45%)	9 (31%)	29	45
E11.5	10 (33%)	14 (47%)	6* (20%)	30	0
E12.0	2	3	0	10	0
				(5 resorptions)	

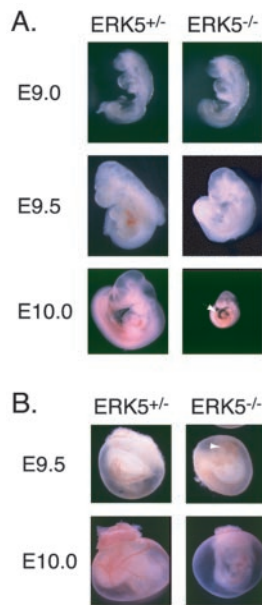


FIG. 2. **Mouse embryos lacking ERK5 exhibit retarded growth and vascular defects in the yolk sacs.** A,  $ERK5^{+/-}$  and  $ERK5^{-/-}$  embryos were dissected out of the yolk sac and amnion at E9.0 (top), E9.5 (middle), or E10.0 (bottom).  $ERK5^{-/-}$  embryos are normal at E9.0 but start appearing smaller and paler at E9.5. At E10.0,  $ERK5^{-/-}$  embryos are much smaller than the control, and  $ERK5^{-/-}$  embryos often exhibit hypotrophic hearts with an enlarged pericardial sac (arrow). B, the yolk sac of an  $ERK5^{-/-}$  embryo at E9.5 (upper panel) displays interconnected vasculature (arrow), which disappears by E10.0 (lower panel), resulting in a smooth and pale appearance.

as the primitive vascular plexus undergoes modification to form rudimentary vessels (data not shown). At E9.5, the endocardium in the hearts of some (~30%)  $ERK5^{-/-}$  embryos appears condensed/collapsed (Fig. 3A, panel d, white arrow). Branching vessels are present in the head, but intersomitic vessels appear shortened, especially in rostral regions (black arrow). Moreover, the endothelial lining of the dorsal aorta begins to assume roughened appearances compared with the controls. At E10, vasculature of  $ERK5^{-/-}$  embryos is extensively disorganized, as characterized by abnormal extensions (especially in the head), improper connections among small vessels and capillaries (panel g, white arrow), and reduction of vessel lumen diameter (black arrow), notably in the primary head veins (Fig. 3A, panels e-g) and dorsal aorta. Intersomitic vessels become progressively less distinct and disorganized toward the caudal region, as further evidenced by discontinuous expression of CD31 outlining the midline dorsal aorta and the ill-defined vascular sinuses that normally branch out from the midline dorsal aorta to form intersomitic vessels (Fig. 3B).

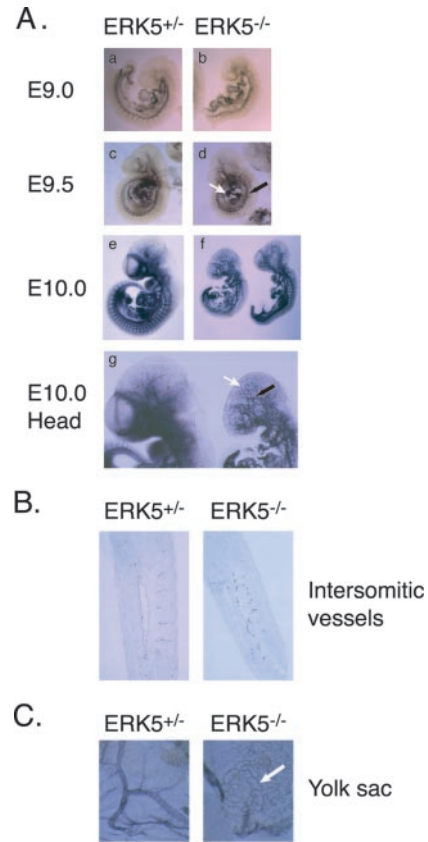


FIG. 3.  **$ERK5^{-/-}$  embryos exhibit vascular defects.** A, whole mount immunohistochemistry to PECAM (CD31) in E9.0, E9.5, and E10.0 embryos indicates that the dorsal aorta and endocardium form in  $ERK5^{-/-}$  embryos, as shown at E9.0 (panels a and b). PECAM expression becomes disorganized starting at E9.5 (panels c and d), with condensed endocardium (panel d, white arrow) and roughened endothelial lining (black arrow), and by E10.0 vascular defects are evident as shown by decreased vessel lumen size and poor remodeling (panels e and f). An enlarged view of the head of the  $ERK5^{+/-}$  (panel g, left) and  $ERK5^{-/-}$  embryos (right) clearly depicts defects in branching, along with improper extensions and interconnections among small vessels (white arrow). The lumen of the head veins is also reduced (black arrow). B, transverse sections of E10.0 embryos stained for PECAM reveal discontinuity in the vascular endothelial lining of the midline dorsal aorta and the lack of branching intersomitic vessels in the  $ERK5^{-/-}$  embryo (right). C, PECAM expression in the  $ERK5^{-/-}$  yolk sac (right) at E10.5 illustrates failure to form large vessels and branching vasculature compared with the  $ERK5^{+/-}$  control (left, see arrow).

The overall levels of CD31 expression (as judged by the staining intensity) do not appear decreased, suggesting that the number of endothelial cells produced in  $ERK5^{-/-}$  embryos is not markedly decreased. Consistent with the initial observation, organization of the  $CD31^{+}$  vascular endothelial cells has

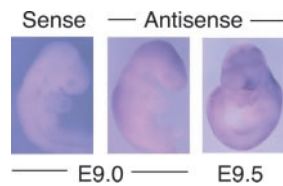


FIG. 4. **Expression of ERK5 is broadly distributed.** *In situ* hybridization of normal embryos using the sense (left) or antisense (middle and right) ERK5 probe indicates that ERK5 is widely expressed. At E9.0, the ERK5 expression is heightened in the head and dorsal regions (middle), and the overall ERK5 expression increases through E9.5 (right).

virtually disappeared in the yolk sacs at E10.5, leaving only a sinuous network of endothelial cells that resembles primitive plexus (Fig. 3C). The ERK5<sup>-/-</sup> yolk sacs tend to contain blood vessels with uniform diameter that are interconnected (white arrow), rather than clearly defined large and branching small vessels as seen in the ERK5<sup>+/-</sup> control yolk sacs. These results suggest that initial vascularization occurs normally but that subsequent remodeling and/or maintenance of vasculature (angiogenesis) is adversely affected in the absence of ERK5.

Analyses by whole-mount *in situ* hybridization indicate that ERK5 expression is not restricted to vascular endothelial cells in wild-type embryos. Rather, ERK5 is expressed broadly, as shown in E9 embryos (Fig. 4), with the highest level of expression in the head and dorsal trunk regions. At E9.5, ERK5 expression increases but remains broadly distributed. We and others previously showed that ERK5 activates the transcription factor MEF2C (30–32). Mice deficient for MEF2C die in midgestation from defects in early heart patterning and vascular abnormalities. Specifically, MEF2C<sup>-/-</sup> embryos fail to initiate looping of the heart tube at E8.5, and they do not develop future right ventricle (35). In contrast, ERK5-deficient embryos undergo normal heart looping from E8.5 through E9, and the left-right specification occurs normally as determined by dHAND (Fig. 5A, panels a and b) and eHAND expression patterns (panels c and d). In Fig. 5A, the ERK5<sup>-/-</sup> heart (panel f) at E9.5 is shown with morphological demarcations corresponding to atrial and ventricular chambers, as well as the bulbus cordis, similarly to the ERK5<sup>+/-</sup> control (panel e). It should be noted that the ERK5<sup>-/-</sup> hearts remain small and immature beyond establishing the basic pattern, and the bulbus cordis region (the future right ventricle) appears particularly hypotrophic. Thus, in some embryos, the future left ventricle appears exaggerated compared with the bulbus cordis and the atrial chambers (Fig. 5A, panel g). The ERK5<sup>-/-</sup> embryonic hearts maintain attenuated trabecular elaboration and hypotrophy of the myocardial walls, especially those surrounding the atrial chamber (panel f, white arrow). In addition, the endocardium appears loosely attached to the outer myocardial walls (panel g, black arrow). Defective trabeculation and retracted endocardium are reminiscent of the phenotype of mice lacking Ang-1 or its receptor Tie-2 (36–38) or mice overexpressing Ang-2 (39).

Mutations that impede vascularization and/or angiogenesis can affect embryonic as well as extraembryonic tissues including placenta. Failure to establish a healthy interface between the embryonic and maternal circulation in the placenta is a frequent cause of embryonic lethality (reviewed in Ref. 40). Disruption of the p38 $\alpha$  MAPK has been shown to cause embryonic lethality starting around E10.5 with defects in both the embryo and placenta (22, 23). In particular, p38 $\alpha$  deficiency results in defective angiogenic invasion of vascular endothelial cells into the labyrinthine layer, which is also reduced in thickness. However, examination of placental sections from E9 and E9.5 embryos revealed no consistent differences in the extent of

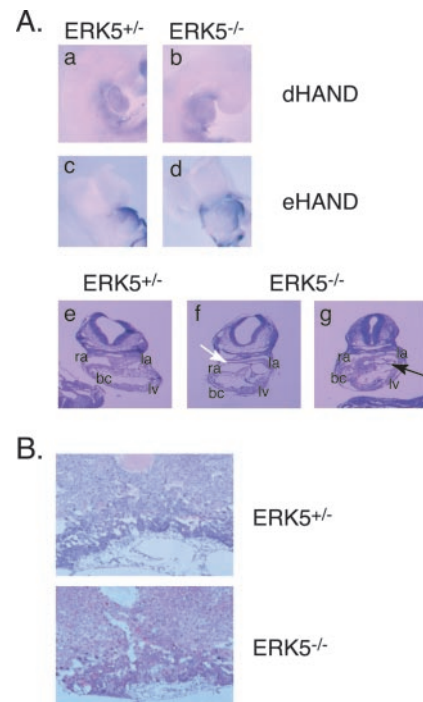
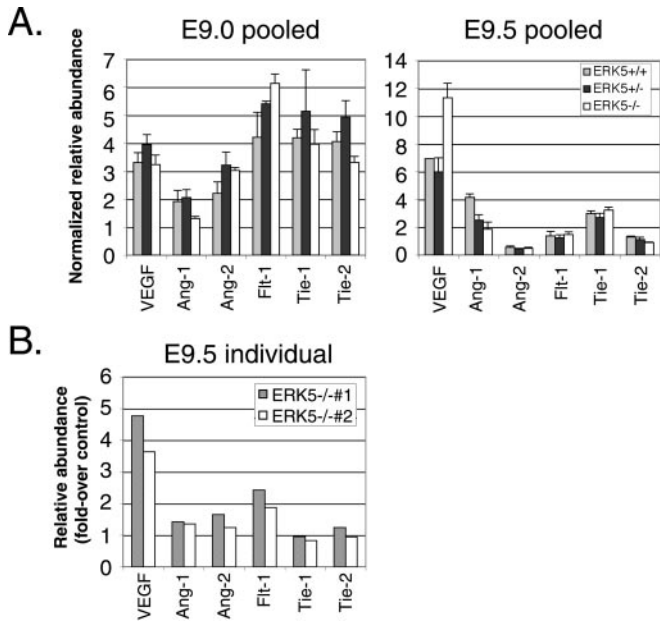


FIG. 5. **ERK5 deficiency does not interfere with heart patterning or placental vascularization at early stages.** A, whole mount *in situ* hybridization analyses indicate that the expression of dHAND at E9.0 (panels a and b) and that of eHAND at E8.5 (panels c and d) are comparable between ERK5<sup>+/-</sup> (panels a and c) and ERK5<sup>-/-</sup> (panels b and d) embryos. Transverse sections of E9.5 embryos indicate that ERK5<sup>-/-</sup> embryos (panels f and g) are able to initiate looping of the linear heart tube and establish the basic structure, including the common atrial chamber (la, left component of the common atrial chamber; ra, right component of the common atrial chamber), future left ventricle (lv), and the bulbus cordis (bc), a structure corresponding to the future right ventricle. In a second ERK5<sup>-/-</sup> embryo (panel g), the bulbus cordis region is smaller and underrepresented. Although the basic pattern is established, the myocardial walls are reduced in thickness (panel f, white arrow), and the endocardium is detached from the myocardium (panel g, black arrow) in ERK5<sup>-/-</sup> embryonic hearts. B, radial sections of E9.5 placental sites stained with hematoxylin and eosin show that the general structures in the ERK5<sup>+/-</sup> (upper panel) and ERK5<sup>-/-</sup> (lower panel) placental sites are comparable.

vascular invasion in the chorionic/ectoplacental plate or in the general architecture of the various layers within the placenta between control and mutant embryos (Fig. 5B). Furthermore, *in situ* hybridization analysis using the eHAND probe (which detects trophoblast cells) indicates that the thickness of the labyrinthine/trophoblast layer in ERK5<sup>-/-</sup> placenta is not significantly altered compared with controls at this stage (data not shown). Since the overt phenotype of ERK5<sup>-/-</sup> embryos is first manifest at around E9.5, when their placenta lack notable defects, we conclude that the earliest defects of ERK5 deficiency arise embryonically rather than as secondary effects of placental defects. At E10, fetal blood vessels are clearly present in the labyrinthine layer of the placenta from ERK5<sup>-/-</sup> embryos, although the diameter of the vessel lumen is reduced (data not shown). These results indicate that ERK5 deficiency eventually affects placental vasculature, which may contribute to the later embryonic phenotypes of ERK5-deficient embryos.

**ERK5 Regulates the Expression of VEGF**—The processes of vascularization and angiogenesis are controlled by multiple growth factors and their receptors, the expression of which is tightly regulated during embryonic development. As previously mentioned, slight deviations in the level or pattern of expression of these proteins result in embryonic lethality due to interference in blood vessel generation and remodeling, as well as in maintaining vessel stability (reviewed in Ref. 10). We



**FIG. 6. Analyses for the expression of vasculogenic and angiogenic factors and their receptors.** *A*, the relative levels of VEGF, Ang-1, Ang-2, Flt-1, Tie-1, and Tie-2 were determined by RT-PCR with total RNA prepared from E9.0 (*left*) or E9.5 (*right*) embryos that were combined by their genotype (+/+, +/-, or -/-). The relative abundance of transcripts was determined in triplicate against individual standard curves, and these values were normalized against  $\gamma$ -actin. The graph summarizes results from a representative experiment ( $n = 3$ ). The error bars indicate S.D. of the triplicate values. *B*, individual E9.5 embryos were analyzed as in *A*, and the values are plotted as -fold over control (ERK5<sup>+/-</sup>) values.

therefore evaluated the expression levels of a panel of genes involved in the control of vasculogenesis and angiogenesis by semiquantitative RT-PCR using the SYBR GREEN™ system. As shown in Fig. 6, analyses of RNA from pooled embryos indicate that the relative abundance of transcripts for VEGF, Ang-1, Ang-2, and their receptors (Flt-1, Tie-2, and Tie-1, respectively) in ERK5<sup>+/-</sup> and ERK5<sup>-/-</sup> embryos are comparable at E9.0 (*left panel*). However, at E9.5, we consistently detected a selective increase in the level of VEGF, and to a lesser extent Flt-1, transcripts in ERK5<sup>-/-</sup> embryos (Fig. 6, *A (right panel)* and *B*). These results were further confirmed when individual embryos were analyzed for expression of these genes (Fig. 6*B*). These data suggest that the absence of functional ERK5 leads to dysregulation of VEGF expression and consequently to the observed angiogenic defects.

It has been shown that VEGF levels increase in response to hypoxia, which plays an important role as an inducer of angiogenesis in tumors and developing embryos (reviewed in Ref. 41). To test whether ERK5 is involved in the induction of VEGF in response to hypoxia, we cultured cells from dissociated, individual E9.5 embryos under normoxic or hypoxic conditions and measured the concentration of secreted VEGF in culture supernatants. As shown previously (42), VEGF secretion is inducible in response to hypoxia (Fig. 7*A*). Moreover, cells from ERK5-deficient embryos produce elevated levels of VEGF compared with those from the control embryos (Fig. 7*A*). The increase is more pronounced with hypoxic treatment of the cells, suggesting that ERK5 may play a role in hypoxia-sensitive regulation of the VEGF expression. Modulation of the VEGF expression has been shown to involve both transcriptional and post-transcriptional mechanisms (reviewed in Ref. 43). To determine whether ERK5 directly regulates the VEGF promoter, we tested VEGF promoter activities in MEF lines derived from the ERK5<sup>-/-</sup> embryos. Utilizing a previously described re-

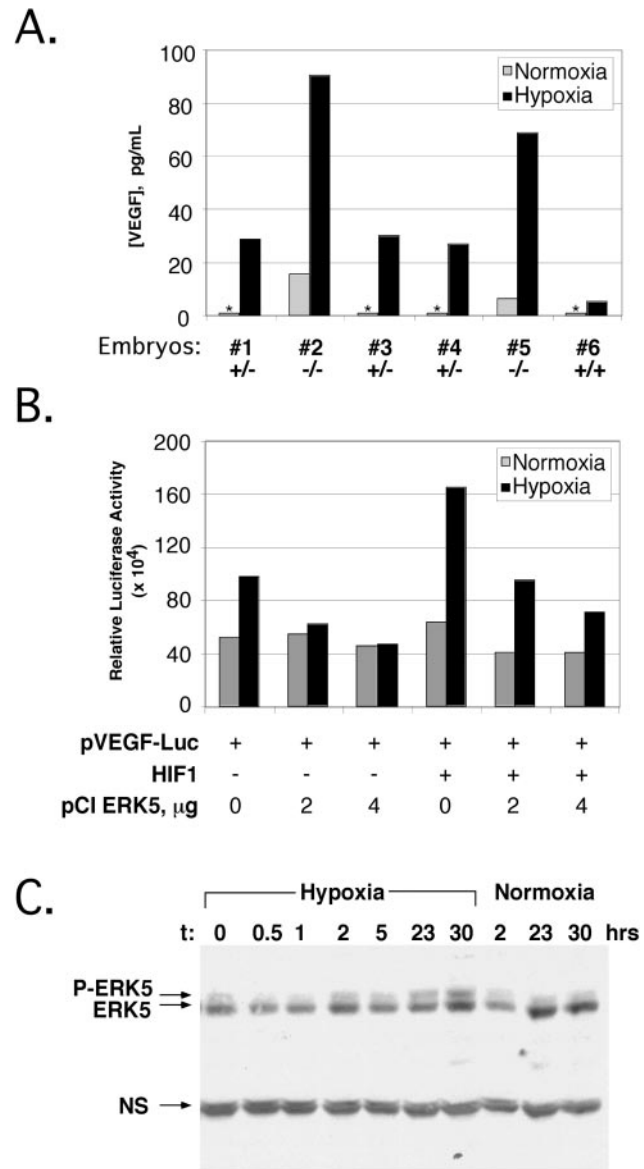


**FIG. 7. ERK5 regulates hypoxia-inducible VEGF expression.** *A*, dissociated cells from E9.5 embryos were cultured under normoxia (gray bars) or hypoxia (black bars), and the concentrations of VEGF in the culture supernatants (that were diluted 1:4 in media) were determined by ELISA. \*, values that were below the detection level. The genotype of each embryo, determined by PCR analyses of the yolk sac genomic DNA and confirmed by anti-ERK5 immunoblotting analyses, is also indicated. The experiment shown is representative of three independent experiments. *B*, the effects of ERK5 on VEGF promoter activity were assessed by a reporter assay. The ERK5<sup>-/-</sup> MEF cells were transiently transfected with the VEGF reporter (pVEGF-Luc) in the presence of increasing doses of ERK5 and cultured under normoxia (gray bars) or hypoxia (black bars). Co-transfection with the components of the HIF-1 transcription factor enhances the hypoxia inducibility of the VEGF promoter, which is repressed by overexpression of ERK5. The experiment shown is representative of three independent experiments. *C*, anti-ERK5 immunoblotting analyses indicate that ERK5 is activated during a hypoxic response in a time-dependent manner. Decreased mobility of the ERK5 proteins (P-ERK5), resulting from phosphorylation and activation, is evident with prolonged exposure to hypoxia but not with exposure to normoxia. NS, a nonspecific signal resulting from antibody cross-reactivity, serving as an internal loading control.

porter system (44, 45), we transfected the ERK5<sup>-/-</sup> MEFs with the full-length VEGF promoter with or without the components of the hypoxia-inducible factor-1 (HIF-1 $\alpha$  and ARNT) in the presence of increasing amounts of exogenous ERK5 and measured the reporter activity in response to hypoxia. Consistent

with previous reports, we found that co-transfection of the HIF-1 components dramatically sensitized the cells for hypoxia-dependent activation of the *vegf* promoter (Fig. 7B). Furthermore, we found that increased expression of ERK5 suppressed hypoxia-inducible activity of the *vegf* promoter (Fig. 7B). Based on these results, we propose that ERK5 acts as a negative regulator in the context of the *vegf* promoter. Finally, we tested whether ERK5 becomes activated in response to hypoxia. To this end, we performed anti-ERK5 immunoblot analyses on MEF cells that had been cultured under hypoxic conditions for various lengths of time. Activation of ERK5 has previously been correlated with decreased mobility in SDS-PAGE (46, 47), and our data clearly demonstrate that exposure to hypoxia induces ERK5 activation within 2 h, with prolonged and continued activation through the 30-h point (Fig. 7C). Longer experiments have indicated that ERK5 returns to resting state by 43 h (the apparent increase in ERK5 levels at 30 h is not observed consistently in other experiments). These results further support our hypothesis that ERK5 plays a role in the regulation of hypoxia-dependent induction of VEGF.

#### DISCUSSION

We have generated ERK5-deficient mice by targeted gene disruption. Heterozygous mutant embryos are viable and develop normally, whereas homozygous-null embryos die around E10.5-E11 (Table I), with notable defects in angiogenesis. ERK5<sup>-/-</sup> embryos (and their yolk sacs and placenta) appear indistinguishable from the control (ERK5<sup>+/+</sup> and ERK5<sup>+/-</sup>) littermates up to E9, with normal cardiogenesis and formation of major blood vessels. The first sign of defects arises at E9.5, when a subset of ERK5<sup>-/-</sup> embryos appears paler and smaller than the controls (Fig. 2A), and PECAM staining reveals condensed endocardium in some, but not all, mutant embryos (Fig. 3A). By E10, all ERK5<sup>-/-</sup> embryos exhibit defects in vascular remodeling and organization in the embryo proper, yolk sacs, and placenta. These embryos are smaller, their yolk sac vasculature appears dissipated (Figs. 2B and 3C and data not shown), and the embryonic blood vessels in the placenta, although present, are reduced in diameter (data not shown). The vascular network in the embryos appears disorganized, particularly in the head (Fig. 3A) and intersomitic vessels (Fig. 3B). The blood vessels in the head are thinner and more uniform in diameter, and vascular endothelial lining of the dorsal aorta is discontinuous. The heart is hypotrophic, often with an enlarged pericardial sac, confirming the failure of embryonic cardiovascular system. Our study suggests that ERK5 deficiency affects the heart later than the stage where MEF2C is required and that early cardiogenesis progresses normally in the absence of ERK5. We postulate that there exists an alternative mechanism of MEF2C activation, perhaps involving a related MAPK p38. Nonetheless, angiogenic defects seen in ERK5<sup>-/-</sup> embryos are reminiscent of the vascular phenotype of MEF2C<sup>-/-</sup> embryos, consistent with the model of ERK5-mediated MEF2C activation.

Deficiency of p38 $\alpha$  results in a strikingly similar phenotype as ERK5 deficiency. p38 $\alpha$ <sup>-/-</sup> embryos also display angiogenic defects, with disorganized vasculature in embryos, yolk sacs, and placenta (22, 23). However, the phenotype of p38 $\alpha$ <sup>-/-</sup> embryos is manifested slightly later compared with ERK5<sup>-/-</sup> embryos, with viable embryos still present after E11.5 when all ERK5<sup>-/-</sup> embryos at this stage are necrotic and resorbing. The similarities shared between the ERK5<sup>-/-</sup> and p38 $\alpha$ <sup>-/-</sup> embryos are consistent with the finding that both MAPKs activate MEF2C. Our results further indicate that the roles of ERK5 and p38 $\alpha$  do not completely overlap *in vivo*, possibly because of the precise timing of their expression and also because they activate MEF2C via distinct mechanisms involving discrete domains found within MEF2C (reviewed in Ref. 48). Moreover,

ERK5 may act on targets distinct from MEF2C that are important for earlier embryonic development.

Consistent with the purported role of Mekk3 as an upstream activator of the MEK5-ERK5 pathway (47), ERK5 deficiency recapitulates many aspects of the Mekk3-deficient embryonic phenotype, including cardiovascular defects and lethality around E11 (49). Although Mekk2 has also been shown to activate ERK5 *in vitro* (50, 51), the finding that the phenotype of ERK5<sup>-/-</sup> mice most closely resembles that of Mekk3<sup>-/-</sup> mice suggests that Mekk3 plays a specific role in activation of the ERK5 pathway during embryogenesis.

The heart phenotype of ERK5<sup>-/-</sup> embryos, including reduction in trabeculation and the thickness of myocardial layer (Fig. 5A), indicates that ERK5 plays a role in ventricular maturation. This phenotype is consistent with the presumed role of ERK5 in neuregulin signaling pathways. In the developing embryonic heart, neuregulins that are present on or secreted from endocardial endothelium bind their cognate receptors expressed on myocardium and induce trabeculation in the ventricles (for a review, see Ref. 52). Thus, the lack of functional ERK5 may block neuregulin signals in the myocardium, leading to the observed defects. Moreover, given the similarities of the heart defects shared by ERK5<sup>-/-</sup>, Ang-1<sup>-/-</sup>, and Tie-2<sup>-/-</sup> embryos, we cannot rule out the possibility that ERK5 regulates Ang-1-dependent signaling pathways.

Analyses of the expression of vasculogenic and angiogenic factors and their receptors indicated that ERK5 deficiency led to a selective increase in the level of VEGF (and potentially its receptor Flt-1; see Fig. 6, A and B) starting around E9.5 (Figs. 6 and 7A). Our data strongly suggest that ERK5 regulates hypoxia-dependent VEGF expression, although basal expression of VEGF may not be as sensitive to changes in total ERK5 activity. Within the context of the embryo, areas of hypoxia presumably play a critical role in regulating local VEGF levels and consequently vascular development. VEGF is a known regulator of vasculogenesis and angiogenesis, and mutations that lead to a modest reduction (6, 7) or increase in VEGF levels (8) are sufficient to interfere with normal vasculogenesis/angiogenesis. Thus, it seems plausible that the increased production of VEGF results in the observed angiogenic defects in ERK5<sup>-/-</sup> embryos.

Interestingly, the MEF2C<sup>-/-</sup> embryos also reportedly produce elevated levels of VEGF at E9.5. In these embryos, hypoxia resulting from compromised circulation and insufficient delivery of oxygen to peripheral tissues was cited as the suspect cause of the VEGF induction. Thus, we considered the possibility that the increased VEGF expression reflects a secondary effect resulting from the vascular defects of ERK5<sup>-/-</sup> embryos. However, three pieces of evidence argue for a direct role of ERK5 in regulating VEGF expression. First, the increased VEGF expression coincides with first signs of vascular defects at E9.5; thus, it seems unlikely that VEGF production increases as a result of general failure in embryonic circulation. Second, hypoxia induces ERK5 activation in MEF cells, suggesting that ERK5 can directly sense changes in oxygen levels in the environment (Fig. 7C). Third, the activity of the *vegf* promoter declines with increasing doses of ERK5 in transfection studies (Fig. 7B).

One mechanism by which transcription of the *vegf* gene is regulated involves transcription factors HIF-1 $\alpha$  and its dimerization partner ARNT. Hypoxia-dependent activation of HIF-1 complex requires increased production and post-translational modification of HIF-1 $\alpha$  proteins (reviewed in Refs. 41 and 43). The fact that ERK5 down-regulates the VEGF promoter activity in cells co-transfected with the HIF-1 components suggests that ERK5 inhibits HIF-1 activity (Fig. 7B). Thus, ERK5 may

play a role as a negative regulator of the HIF-1 transcription factor, although this needs to be studied further.

The phenotypes of the ERK5<sup>-/-</sup> embryos suggest that ERK5 regulates multiple signaling pathways involved in angiogenesis and heart maturation. Our study alludes to a mechanism of angiogenic regulation whereby ERK5 inhibits the expression of VEGF during hypoxic responses, potentially via an undefined feedback mechanism. Additional studies will further clarify the role of this MAPK in angiogenesis during development as well as in cancer models.

**Acknowledgments**—We thank Dr. M. Rubinstein for sending the pVEGF-Luc (from B. Z. Levi) and pcDNA3-ARNT (E. Huang) plasmids, Dr. G. Semenza for the gift of pCEP4 HIF-1 $\alpha$ , and Dr. E. Olson for the eHAND and dHAND probes. We are indebted to Dr. W. Skarnes and the members of the Skarnes laboratory for helpful discussions, Drs. O. Kelly and A. Chavez-Reyes for technical advice, and Drs. J. Reiter and L. Lenz for critical reading of the manuscript. We also thank L. Hsing for assistance in maintaining the mouse colony.

**Addendum**—While this manuscript was in preparation, another report describing the disruption of the *erk5* gene was published (53). The phenotypes of ERK5<sup>-/-</sup> embryos in this report are similar to ours, with the exception of two points of discrepancy. First, we believe that ERK5 deficiency affects heart development at later stages, since the looping and the left-right specification occur normally in our ERK5<sup>-/-</sup> embryos. Second, ERK5 deficiency leads to an increased expression of VEGF in our system, which we further investigated through additional studies.

## REFERENCES

- Beck, L., Jr., and D'Amore, P. A. (1997) *FASEB J.* **11**, 365–373
- Risau, W. (1997) *Nature* **386**, 671–674
- Pardanaud, L., Yassine, F., and Dieterlen-Lievre, F. (1989) *Development* **105**, 473–485
- Baldwin, H. S. (1996) *Cardiovasc. Res.* **31**, E34–E45
- Patan, S. (2000) *J. Neurooncol.* **50**, 1–15
- Carmeliet, P., Ferreira, V., Breier, G., Pollefeijt, S., Kieckens, L., Gertsenstein, M., Fahrig, M., Vandenhoek, A., Harpal, K., Eberhardt, C., Declercq, C., Pawling, J., Moons, L., Collen, D., Risau, W., and Nagy, A. (1996) *Nature* **380**, 435–439
- Ferrara, N., Carver-Moore, K., Chen, H., Dowd, M., Lu, L., O'Shea, K. S., Powell-Braxton, L., Hillan, K. J., and Moore, M. W. (1996) *Nature* **380**, 439–442
- Miquerol, L., Langille, B. L., and Nagy, A. (2000) *Development* **127**, 3941–3946
- Dvorak, H. F., Nagy, J. A., Feng, D., Brown, L. F., and Dvorak, A. M. (1999) *Curr. Top. Microbiol. Immunol.* **237**, 97–132
- Yancopoulos, G. D., Davis, S., Gale, N. W., Rudge, J. S., Wiegand, S. J., and Holash, J. (2000) *Nature* **407**, 242–248
- Carmeliet, P., Mackman, N., Moons, L., Luther, T., Gressens, P., Van Vlaenderen, I., Demunck, H., Kasper, M., Breier, G., Evrard, P., Muller, M., Risau, W., Edgington, T., and Collen, D. (1996) *Nature* **383**, 73–75
- Hellstrom, M., Kalen, M., Lindahl, P., Abramsson, A., and Betsholtz, C. (1999) *Development* **126**, 3047–3055
- Alon, T., Hemo, I., Itin, A., Pe'er, J., Stone, J., and Keshet, E. (1995) *Nat. Med.* **1**, 1024–1028
- Pierce, E. A., Foley, E. D., and Smith, L. E. (1996) *Arch. Ophthalmol.* **114**, 1219–1228
- Stone, J., Chan-Ling, T., Pe'er, J., Itin, A., Gnessin, H., and Keshet, E. (1996) *Invest. Ophthalmol. Vis. Sci.* **37**, 290–299
- Holash, J., Wiegand, S. J., and Yancopoulos, G. D. (1999) *Oncogene* **18**, 5356–5362
- Cobb, M. H. (1999) *Prog. Biophys. Mol. Biol.* **71**, 479–500
- Pages, G., Guerin, S., Grall, D., Bonino, F., Smith, A., Anjuere, F., Auburger, P., and Pouyssegur, J. (1999) *Science* **286**, 1374–1377
- Dong, C., Yang, D. D., Wisk, M., Whitmarsh, A. J., Davis, R. J., and Flavell, R. A. (1998) *Science* **282**, 2092–2095
- Yang, D. D., Conze, D., Whitmarsh, A. J., Barrett, T., Davis, R. J., Rincon, M., and Flavell, R. A. (1998) *Immunity* **9**, 575–585
- Kuan, C. Y., Yang, D. D., Samanta Roy, D. R., Davis, R. J., Rakic, P., and Flavell, R. A. (1999) *Neuron* **22**, 667–676
- Mudgett, J. S., Ding, J., Guh-Siesel, L., Chartrain, N. A., Yang, L., Gopal, S., and Shen, M. M. (2000) *Proc. Natl. Acad. Sci. U. S. A.* **97**, 10454–10459
- Adams, R. H., Porras, A., Alonso, G., Jones, M., Vintersten, K., Panelli, S., Valladares, A., Perez, L., Klein, R., and Nebreda, A. R. (2000) *Mol. Cell* **6**, 109–116
- Tamura, K., Sudo, T., Senftleben, U., Dadak, A. M., Johnson, R., and Karin, M. (2000) *Cell* **102**, 221–231
- Kato, Y., Kravchenko, V. V., Tapping, R. I., Han, J., Ulevitch, R. J., and Lee, J. D. (1997) *EMBO J.* **16**, 7054–7066
- Kato, Y., Tapping, R. I., Huang, S., Watson, M. H., Ulevitch, R. J., and Lee, J. D. (1998) *Nature* **395**, 713–716
- Cavanaugh, J. E., Ham, J., Hetman, M., Poser, S., Yan, C., and Xia, Z. (2001) *J. Neurosci.* **21**, 434–443
- Watson, F. L., Heerssen, H. M., Bhattacharyya, A., Klesse, L., Lin, M. Z., and Segal, R. A. (2001) *Nat. Neurosci.* **4**, 981–988
- Esparis-Ogando, A., Diaz-Rodriguez, E., Montero, J. C., Yuste, L., Crespo, P., and Pandiella, A. (2002) *Mol. Cell. Biol.* **22**, 270–285
- Kato, Y., Zhao, M., Morikawa, A., Sugiyama, T., Chakravorty, D., Koide, N., Yoshida, T., Tapping, R. I., Yang, Y., Yokochi, T., and Lee, J. D. (2000) *J. Biol. Chem.* **275**, 18534–18540
- Kasler, H. G., Victoria, J., Duramad, O., and Winoto, A. (2000) *Mol. Cell. Biol.* **20**, 8382–8389
- Yang, C. C., Ornatsky, O. I., McDermott, J. C., Cruz, T. F., and Prody, C. A. (1998) *Nucleic Acids Res.* **26**, 4771–4777
- Ausubel, F. M. (1988) *Current Protocols in Molecular Biology*, Greene Publishing/Wiley-Interscience, New York
- Hogan, B. (1994) *Manipulating the Mouse Embryo: A Laboratory Manual*, 2nd Ed., Cold Spring Harbor Laboratory, Cold Spring Harbor, NY
- Lin, Q., Schwarz, J., Bucana, C., and Olson, E. N. (1997) *Science* **276**, 1404–1407
- Patan, S. (1998) *Microvasc. Res.* **56**, 1–21
- Sato, T. N., Tozawa, Y., Deutsch, U., Wolburg-Buchholz, K., Fujiwara, Y., Gendron-Maguire, M., Gridley, T., Wolburg, H., Risau, W., and Qin, Y. (1995) *Nature* **376**, 70–74
- Suri, C., Jones, P. F., Patan, S., Bartunkova, S., Maisonpierre, P. C., Davis, S., Sato, T. N., and Yancopoulos, G. D. (1996) *Cell* **87**, 1171–1180
- Maisonpierre, P. C., Suri, C., Jones, P. F., Bartunkova, S., Wiegand, S. J., Radziejewski, C., Compton, D., McClain, J., Aldrich, T. H., Papadopoulos, N., Daly, T. J., Davis, S., Sato, T. N., and Yancopoulos, G. D. (1997) *Science* **277**, 55–60
- Ihle, J. N. (2000) *Cell* **102**, 131–134
- Dor, Y., Porat, R., and Keshet, E. (2001) *Am. J. Physiol.* **280**, C1367–C1374
- Shweiki, D., Itin, A., Soffer, D., and Keshet, E. (1992) *Nature* **359**, 843–845
- Semenza, G. L. (2001) *J. Clin. Invest.* **108**, 39–40
- Forsythe, J. A., Jiang, B. H., Iyer, N. V., Agani, F., Leung, S. W., Koos, R. D., and Semenza, G. L. (1996) *Mol. Cell. Biol.* **16**, 4604–4613
- Zelzer, E., Levy, Y., Kahana, C., Shilo, B. Z., Rubinstein, M., and Cohen, B. (1998) *EMBO J.* **17**, 5085–5094
- Abe, J., Takahashi, M., Ishida, M., Lee, J. D., and Berk, B. C. (1997) *J. Biol. Chem.* **272**, 20389–20394
- Chao, T. H., Hayashi, M., Tapping, R. I., Kato, Y., and Lee, J. D. (1999) *J. Biol. Chem.* **274**, 36035–36038
- McKinsey, T. A., Zhang, C. L., and Olson, E. N. (2002) *Trends Biochem. Sci.* **27**, 40–47
- Yang, J., Boerm, M., McCarty, M., Bucana, C., Fidler, I. J., Zhuang, Y., and Su, B. (2000) *Nat. Genet.* **24**, 309–313
- Garrington, T. P., Ishizuka, T., Papst, P. J., Chayama, K., Webb, S., Yujiri, T., Sun, W., Sather, S., Russell, D. M., Gibson, S. B., Keller, G., Gelfand, E. W., and Johnson, G. L. (2000) *EMBO J.* **19**, 5387–5395
- Sun, W., Kesavan, K., Schaefer, B. C., Garrington, T. P., Ware, M., Johnson, N. L., Gelfand, E. W., and Johnson, G. L. (2001) *J. Biol. Chem.* **276**, 5093–5100
- Brutsaert, D. L., Fransen, P., Andries, L. J., De Keulenaer, G. W., and Sys, S. U. (1998) *Cardiovasc. Res.* **38**, 281–290
- Regan, C. P., Li, W., Boucher, D. M., Spatz, S., Su, M. S., and Kuida, K. (2002) *Proc. Natl. Acad. Sci. U. S. A.* **99**, 9248–9253